www.czasopisma.pan.pl PAN POLSKA AKADEMIA NAUK www.journals.pan.pl

Acta Geologica Polonica, Vol. 69 (2019), No. 3, pp. 465–488
DOI: 10.24425/agp.2019.126442

Microstructural changes of expansive clays during dehydration caused by suction pressure – a case study of Miocene to Pliocene clays from Warsaw (Poland)

EMILIA WÓJCIK[1], JERZY TRZCIŃSKI[2] and KATARZYNA ŁĄDKIEWICZ-KROCHMAL[1]

[1] *Faculty of Geology, University of Warsaw, Żwirki i Wigury 93, PL-02-089 Warszawa, Poland.*
E-mails: wojcike@uw.edu.pl; katarzyna_ladkiewicz@wp.pl
[2] *Wroclaw Research Centre EIT+, Stabłowicka 147, PL-54-066 Wrocław, Poland.*
E-mail: jerzy.trzcinski@uw.edu.pl

ABSTRACT:

Wójcik, E., Trzciński, J. and Łądkiewicz-Krochmal, K. 2019. Microstructural changes of expansive clays during dehydration caused by suction pressure – a case study of Miocene to Pliocene clays from Warsaw (Poland). *Acta Geologica Polonica*, **69** (3), 465–488. Warszawa.

This paper presents the qualitative and quantitative characteristics of microstructures of Neogene clays from Warsaw, Poland. Scanning Electron Microscope (SEM) studies were used for the microstructural analysis of natural clays and clay pastes. Qualitative microstructural changes were observed: from a honeycomb microstructure for the initial clay paste to a turbulent microstructure for the dried paste. It was also noticed that water loss caused by the increase of the suction pressure had a significant impact on the microstructural transformations. Significant changes in the quantitative values of the pore space parameters were also observed. Increase of suction pressure and water loss caused a decrease in porosity and changes in the values of morphometric parameters, such as pore distribution; for example, a significant increase of the number of pores of 0−10 μm size and changes in the geometric parameters of the pore space were noticed with the increase of suction pressure. The pore space with larger isometric pores was modified into a pore space with the dominance of small anisometric and fissure-like pores. The increased degree of anisotropy from a poorly-oriented to a highly-oriented microstructure was also observed. After rapid shrinkage the reduction in the number of pores, maximum pore diameter, and total pore perimeter was recorded. The process of rapid water loss induced the closure of very small pores. A similar effect was observed during the increase of the suction pressure, where the closure of pore space of the clay pastes was observed very clearly.

Key words: Clay pastes; Quantitative image analyses; Pore space; Soil-water curve.

INTRODUCTION

The most significant aspects of geotechnical engineering should be analyzed taking into account the types and behaviours of soil. A number of issues commonly occurring during civil engineering building projects are typically associated with the changes in water content near the ground surface (in the upper few metres) and are influenced by various environmental factors: natural (precipitation, high temperatures, frost) and anthropogenic (pollution). The zone that comprises the soil thickness and is correlated with the environmental conditions is generally termed the active zone; negative pore water pressure, also known as suction pressure, occurs in this zone. In the unsaturated state, the relationship

between moisture change and soil volume change is affected by factors such as the soil structure and the moisture content-suction relationship.

The most important element of the behaviour of unsaturated soil is the relationship between water and air (as soil desaturates). This relationship is described as the Soil-Water Characteristic Curve (SWCC). The Soil-Water Characteristic Curve contains key information such as pore size distribution, amount of water contained in the pores at any level of suction, and the stress state. An unsaturated soil consists of more than two phases and therefore the laws governing its behaviour change relative to conventional saturated soil mechanics. Modern soil mechanics assumes the existence of an air phase and a water phase with an air-water interface in the pores. Properties of soils such as void ratio, water content (moisture), or degree of saturation are correlated with the distribution of particles and pores, their size, shape and distribution, all of which determine the soil properties. In unsaturated soils, beside the pore space parameters, the properties of soils depend on the states of stresses and strains. The concept of structure and especially microstructure is closely related with these issues.

There are many definitions of the structure used in geosciences and they differ depending on which branch of geology they are used for. In the study of clays the structure is used as a complex term due to their character and degree of diagenesis. In engineering geology the definition of the structure of clays comprises three elements: (i) grain size and mineral composition; (ii) fabric, referring to the composition, shape and size of the structural elements of the skeleton and the character of the pore space (porosity, pore size and shape, pore distribution); and (iii) forces between the structural elements of the soil skeleton (Mitchell 1976; Gillott 1987).

The influence of microstructure (the structure that is studied with a SEM) on the behaviour of clays has been studied and reported in the past in many soil engineering research publications (e.g., Gillott 1970, 1979; Pusch 1966, 1970; Collins and McGown 1974; McGown and Collins 1975; Grabowska-Olszewska 1975; Murphy *et al.* 1977; Delage and Lefebvre 1984; Bennett *et al.* 1991). The understanding of the structural and microstructural properties is indispensable in any sort of interpretation of soil origin and dynamics of postdepositional changes (Grabowska-Olszewska 1998). Moreover, the study of microstructure transformations is crucial, not only in the understanding of the mechanisms of hydration or dehydration of structural elements of the soil skeleton (particles, microaggregates, aggregates and grains), but also in the interpretation of mechanical soil properties such as strength and compressibility. Studies of these are particularly important for engineering and geotechnical applications.

The increasing application of microstructural studies has led to improved techniques and more robust interpretations of the results. At present, most of the SEM studies are devoted to the determination of the size and orientation of pores and their evolution under various conditions of stress on consolidation, compaction or shearing paths (e.g., Osipov and Sokolov 1978a, b, c; Osipov *et al.* 1984; Sokolov 1990; Gens and Alonso 1992; Hicher *et al.* 2000; Katti and Shanmugasundaram 2001; Yong 2003; Dananaj *et al.* 2005; Schmitz *et al.* 2005; Gratchev *et al.* 2006; Hattab *et al.* 2010; Hattab and Fleureau 2010, 2011).

The use of computer techniques coupled with specialized software allows for the enhanced abilities of these studies and for, not only qualitative, but also quantitative microstructural parameters (including parameters of pore space) of the clay structure to be assessed (e.g., Sergeyev *et al.* 1984a, b; Kaczyński 2000, 2001, 2003; Sokolov *et al.* 2002; Ruszczyńska-Szenajch *et al.* 2003; Trzciński 2004; Izdebska-Mucha and Trzciński 2008; Izdebska-Mucha *et al.* 2011). Understanding the microstructural behaviour of clays has a particular relevance in geotechnical applications, therefore more enhanced methodologies for studying and quantifying the arrangements of aggregations/particles and pore space in unsaturated soils has become very important. ESEM (environmental scanning electron microscopy) is capable of creating such opportunities. It works under controlled environmental conditions and is applied in studies of geological materials such as those reported e.g., by Romero *et al.* (1999), Villar and Lloret (2001), Agus and Schanz (2005), Viola *et al.* (2005), and Zhang *et al.* (2005).

Studies concerning the effect of suction on the microstructure of clay soils are much less frequent. MIP (Mercury Intrusion Porosimetry) results have been used to predict, among others, the water retention properties (e.g., Romero *et al.* 1999; Simms and Yanful 2002, 2005) as well as macroscopic volume changes that are the effects of mechanical and hydraulic paths (e.g., Simms and Yanful 2004; Cuisinier and Laloui 2004; Lloret *et al.* 2004; Romero *et al.* 2005; Koliji *et al.* 2006). Simms and Yanful (2001, 2002) measured the PSD (Pore Size Distribution) during water retention curve tests on compacted clay soils and proved that PSD changed significantly not only in the distribution but also in the total volume of pores. Evolution of the orientation of the clay par-

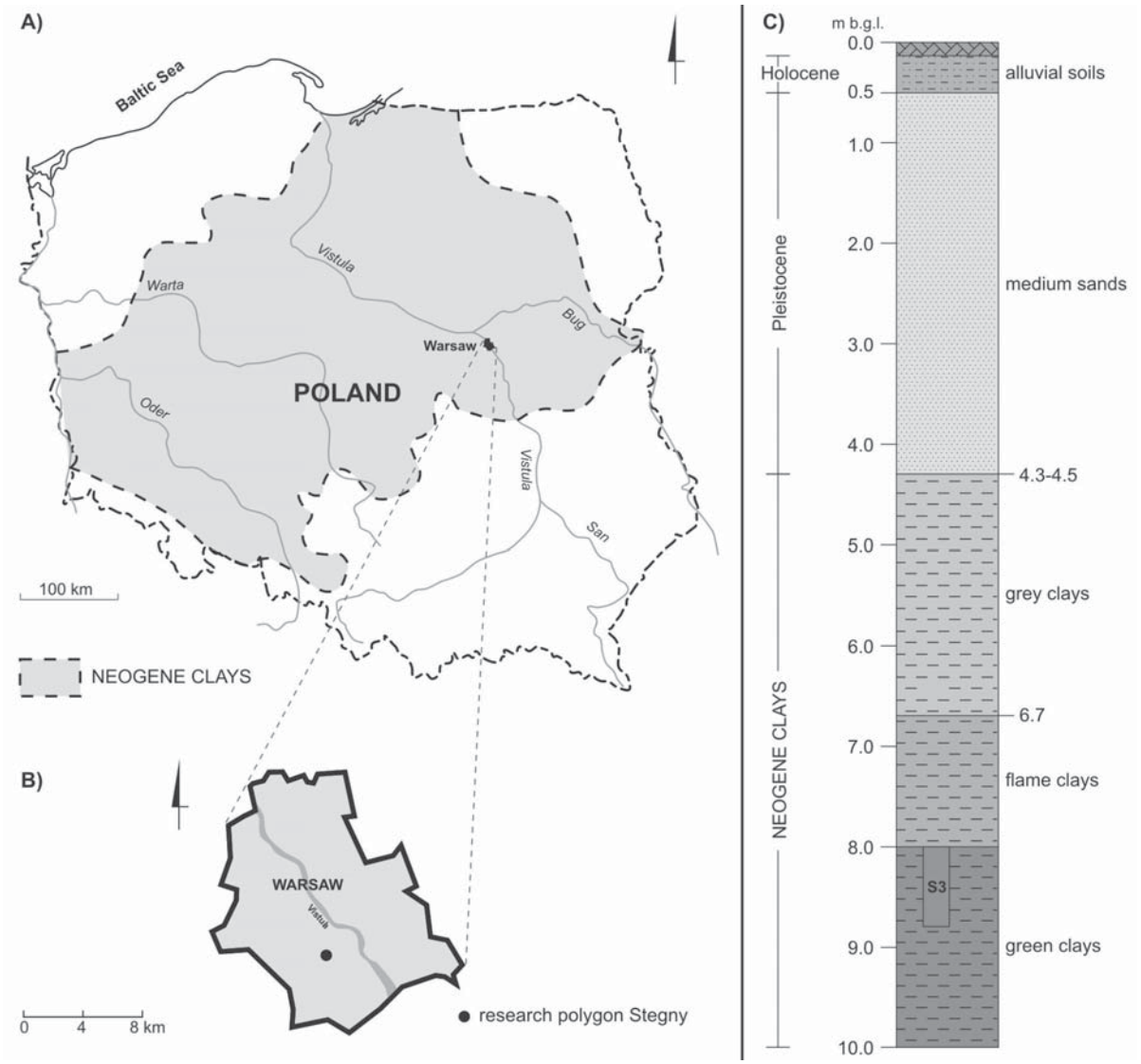

Text-fig. 1. Location of the study area with: A – extension of Neogene clays in Poland; B – boundaries of Warsaw; C – lithological succession of the test drilling from the study locality

ticles performed under different suctions for two clay materials – kaolinite and a mixture of kaolinite and montmorillonite – were presented by Wei *et al.* (2013). Using SEM and MIP these authors found that when suction increases, pores are affected with a reduction of the pore diameter and volume. A combination of MIP analyses and SEM observations was used also by Seiphoori *et al.* (2014) during their study of drying-wetting cycles on the microstructure of bentonite. Geremew *et al.* (2009) studied the effect of the hydraulic path on the microstructure of a natural soil. Similarly, the results of the observations of the microstructure of natural soils resulting from the state of load and deformation – specifically Neogene clays from the vicinity of Warsaw – using a conventional SEM were presented by Kaczyński (2000, 2001, 2003). The present study, besides focusing on the characteristics of the microstructure aspects and quantitative microstructural analysis of Neogene clays from the Stegny locality in Warsaw, focuses on the microstructural evolution of the material as a function of its hydration state on a drying path.

At the microscopic scale, the study of the orientation of the clay particles and the pore diameter

distribution were carried out by SEM picture analysis under different suctions, whereas at the macroscopic scale, the approach consisted of measurements of the water content versus suction during drying. The understanding of the actual water content at a particular level of suction and the parameters of the consistency of the studied soil allowed us to assign them into a particular type of microstructure and to trace their evolution at different hydration states. Simultaneously, the results of microstructure obtained for the tested soil were referred to actual parameters, which describe the basic physical properties of clays (i.e., liquidity index – I_L).

DESCRIPTION OF THE SITE AND ITS GEOLOGICAL HISTORY

The natural clays used as the basis of this study were obtained from Warsaw, Mazowsze province, in Central Poland. This is the area with common shallowly occurring Miocene to Pliocene clays of the Poznań series, which are characterized by expansive properties (Kaczyński and Grabowska-Olszewska 1997; Kumor 2008, 2016). These clays cover a vast area of Poland and are overlain by Quaternary drift deposits of varying thickness. The clays of the Poznań series are dated to the Neogene and developed from the middle Miocene to the early Pliocene (Piwocki 2002). The series is lithologically varied, and includes clays and subordinate silty-sandy sediments ranging across the entire area of the Polish Lowlands (Text-fig. 1A). The clays originated in an extensive and shallow, inland water basin, and are characterized by three lithostratigraphic levels differing by the sedimentary environment, the geochemical conditions and the varied mineral content. The lower level comprising grey clays formed in a swampy environment, the middle level – green clays – formed in reducing conditions, whereas the upper level – known as the 'sunburnt' clays formed in oxidizing conditions (Dyjor 1992). The thickness of the clays of the Poznań series varies. The maximum primary thickness is estimated at 150 m in the central region (Frankowski and Wysokiński 2000). Both the thickness and the depth at which the clays presently occur were influenced by glaciotectonic processes and it is clear through the observation of wide folds and brittle deformations that these clays are highly glaciotectonically disturbed (Brykczyńska and Brykczyński 1974).

As a result, the clays around Warsaw have a varying thickness of 50–150 m. In the field, they occur below a thin cover of Quaternary deposits or directly on the surface. From an engineering point of view, the shallow occurrence of the clays allows for understanding of their properties to solve the problem of foundation on expansive soil. In Warsaw, these soils occur close to the ground level in the Stegny district (Text-fig. 1B); the clays attain a thickness of 142 m and occur directly below a 4 m thick layer of alluvial sands (Kaczyński *et al.* 2000). The water-soil conditions have been established by CPTU (Piezocone Penetration Tests) soundings to the depth of 46 m bgl. Monitoring of the distribution of pore pressure in the piezometers was performed from 2002 to the present (pers. comm. Barański 2015). The Stegny locality was chosen for this research since it has been well documented prior to this study (Kaczyński *et al.* 2000; Bajda 2002; Sobolewski 2002; Wójcik 2003; Barański *et al.* 2004, 2009; Lech and Bajda 2004; Szczepański 2005; Barański and Wójcik 2007, 2008; Izdebska-Mucha and Wójcik 2014). However, none of the previous research related to the assessment of the effect of soil suction on the microstructure of the studied clays.

This paper focuses on the study of the middle lithostratigraphic level of Neogene green clays, sampled at Stegny locality in Warsaw (Central Poland). An undisturbed soil sample was collected from a drilling from the depth of 8.0–8.7 m and is marked as sample S3 (Text-fig. 1C) and hereafter called 'natural' (Table 1).

Parameter		Sample symbol	
		Clay – natural specimen	Clay pastes
Grain size	sand (2–0.05 mm) f_p [%]	–	9
	silt (0.05–0.002 mm) f_π [%]	37	31
	clay (<0.002 mm) f_i [%]	63	60
Water content w_n [%]		27.5	78.3*
Solid density ρ_s [Mg/m^3]		2.71	2.66
Wet/bulk density ρ [Mg/m^3]		2.05	–
Dry density ρ_d [Mg/m^3]		1.61	–
Porosity n [%]		40.6	–
Void ratio e [–]		0.69	–
Plastic limit w_P [%]		22.5	24.0
Liquid limit w_L [%]		69.5	68.3
Plasticity index I_P [%]		47.0	44.3
Liquidity index I_L [–]		0.11	1.23
Shrinkage limit w_S [%]		12.3	11.4
Degree of saturation S_r [–]		1.0	–
Activity A [–]		0.75	0.70

Table 1. Selected geological and engineering properties of the Miocene to Pliocene clays and clay pastes (initial) from the Stegny locality in Warsaw; * initial water content of clay pastes

METHODOLOGY OF RESEARCH

Grain size composition and measurements of the physical parameters of the clays were performed in compliance with PN-88/B-04481 and PN-86/02480 norms. The mineral content was determined based on the X-ray powder diffraction (XRD) using the Panalytical X'Pert PRO MPD X-ray diffractometer (Kulesza-Wiewióra 1990). The conditions included: a cobalt lamp, the range of the angle measurement of 0–57°, a 2Theta step size of 0.026°, the awakening pressure of 40 kV, and an electric current of 30 mA. Additionally, determinations of the mineral content were performed using differential thermal analyses (DTA) using a Q600 instrument from TA Instruments and applying the methodology developed by Wyrwicki and Kościówko (1996).

Specimen preparation and testing details

A comparative review of the literature shows that three types of samples: undisturbed (natural), remolded and compacted, are used in the experimental studies of soils. Soils prepared by remolding or compaction have an entirely different structure, and therefore different composition and pore size distribution, to that observed in natural soils, with the differences being particularly significant in clay soils (Fityus and Buzzi 2009).

The natural clays of the Poznań series are inhomogeneous and anisotropic. Therefore, soils prepared from slurry were used for this study. Crumbled clays were air-dried and pounded in an agate mortar, and later sieved through a 100 μm sieve. In order to saturate the samples, de-aired water was mixed with the soil powders to make (perfectly) homogenic slurries without lumps with an initial water content $w = w_L \div 1.5w_L$ (where w_L is the liquid limit). This procedure follows the methodology described by Burland (1990). The slurry was then inserted into metal cylinders and secured from drying, and subjected to a consolidation process for 2 months in unconfined conditions under a weight of 30 kPa (initial paste). The resedimented sample was sub-divided into smaller cylindrical specimens of diameter 54 mm and height 40 mm. This enabled to prepare fully saturated soil samples with a unified pore size distribution. Starting from a saturated and structurally isotropic initial state, this allowed the analyses of actual microstrutural changes, whereas the soils were submitted to drying under different controlled values of suction.

Samples obtained in this way were placed in a large 5 bar and 15 bar pressure plate extractor (Soilmoisture Equipment Corporation, model 1500). The moisture tension results were obtained by creating a series of over-pressures of 50, 100, 200, 250, 300, 400, 1600 kPa. After each pressure increment, sustained for about two weeks in order to obtain equilibrium, the samples were removed and weighed. Due to the high structural sensitivity of clays, immediately after each stage a small amount of the soil was trimmed from the test specimen for microstructural analyses. The remaining samples were then placed again in the instrument and incurred a further pressure increment.

The weighing of the sample was undertaken after each balance adjustment and the dry mass was obtained after the completion of the test yields including the moisture content for each moisture tension. Moreover, an air dried sample was taken at the end of each cycle of examinations and further dried again at 105°C. Duplicate samples from each stage were analysed, and the results including the quantitative characteristics of the pore space parameters that are presented below are based on averaged results. In order to obtain the full structural characteristics of the material used for the particular analyses, a series of samples was compared: natural sample, initial paste, pastes on which suction pressure was imposed in stages, and shrunken sample dried according to the procedure of linear shrinkage L_s assessment (BS 1377-2:1990:6.5).

For the microstructural analyses rectangular cuboid samples of approximately 1 cm^3 volume were cut out, frozen and dried using the freeze-drying method (Tovey and Wong 1973; Osipov and Sokolov 1978a, b; Smart and Tovey 1982; Trzciński 2004). During shock freezing in liquid nitrogen the pore water turned into vitrified ice. Vacuum drying was performed under a pressure of 10^{-3}–10^{-5} Pa. When the sample freeze level was maintained in the temperature range of -50 to -60°C, the ice started to undergo a slow sublimation. The freeze-drying method allowed the prevention of shrinking during the drying of clays, thus keeping its structure intact; as a result, the actual parameters of the microstructure could be analyzed. After drying, a fresh surface was exposed by breaking the sample. It was cleaned by the peeling method and powdered with a layer of carbon, and a platinum and gold alloy. Samples prepared in such way were then used for microstructural analyses.

Microstructural analyses

Observations of the sample surfaces for the purpose of qualitative analyses were performed with a

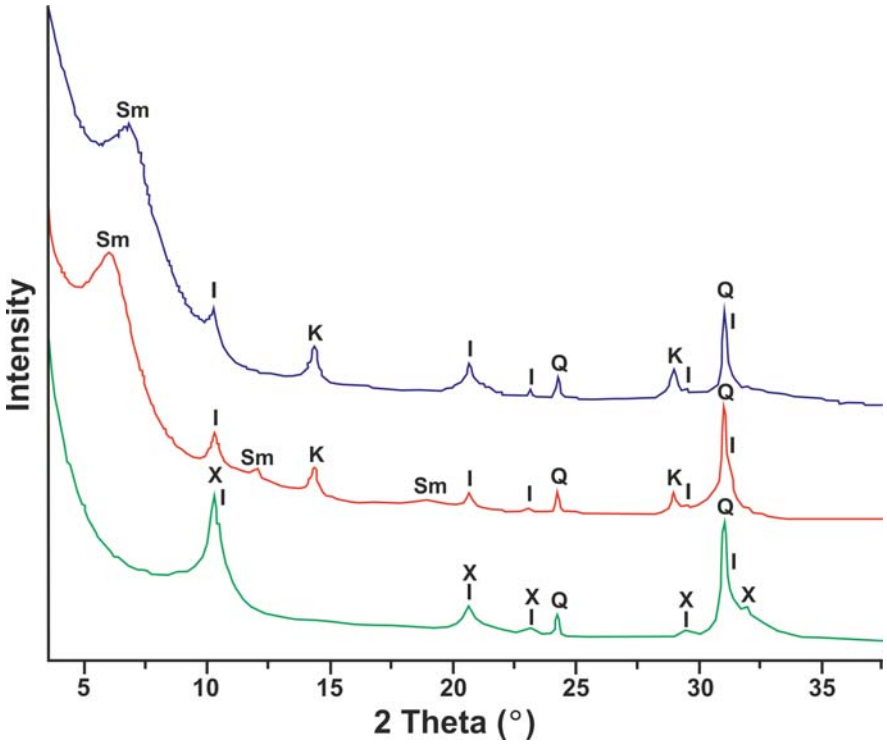

Text-fig. 2. XRD diffractograms for clays from the Stegny locality. Sm – smectite, I – illite, K – kaolinite, Q – quartz, X – crystalline phase similar to mica group, blue line – sample after ethylene glycol treatment, red line – sample after sedimentation, green line – sample after heat treatment

JEOL Scanning Electron Microscope (SEM), model JSM 6380 LA. The secondary electrons signal (SE), depending on the microtopography of the surface, was used. The chosen microscopic regime allowed for obtaining images with sharp boundaries between the structural elements (such as grains and particles) and the pores. The type of the microstructure, the elements of the structural skeleton, the degree of packing, the types of contacts between the pores, and the characteristics of the pore space were recorded using the terminology and classification of clay microstructures by Sergeyev *et al.* (1978, 1980) and Grabowska-Olszewska *et al.* (1984).

Quantitative analyses were performed using specialist image analysis software STIMAN (STructural IMage Analysis) for quantitative morphological analyses based on SEM images (Sergeyev *et al.* 1984a, b; Sokolov *et al.* 2002; Trzciński 2004). They allowed for the determination of the morphometric and geometric parameters of the pore space. Six analyses were performed for each sample and the results were averaged. The analyses were performed based on a series of images using magnifications of 200 to 6500 times. The quantitative analysis was performed based on the software manual (Sokolov *et al.* 2002). The quantitative analyses were performed in the Scanning Electron Microscopy and Microanalyses Laboratory, Faculty of Geology, University of Warsaw.

The analyses of SEM images allowed for the definition of pore space parameters: area S, perimeter P, diameter D, pore form index K_f, and degree of orientation of the structural elements – the microstructural anisotropy index K_a. Based on pore size distribution, the contribution of micropores of Ø 0.1–10 µm and of mesopores of Ø 10–1000 µm was determined (Grabowska-Olszewska *et al.* 1984). Index K_f allows for the determination of three categories of pore shapes (Sokolov *et al.* 2002):

– isometric pores at K_f 1–0.66 (the ratio of two extreme measurements a/b being lower than 1.5),
– anisometric pores at K_f 0.66–0.1 (the ratio of two extreme measurements a/b being between 1.5 and 10),
– fissure-like pores at K_f 0.1–0 (ratio of two extreme measurements a/b being higher than 10).

The degree of orientation of the structural elements was determined using the decrease in signal

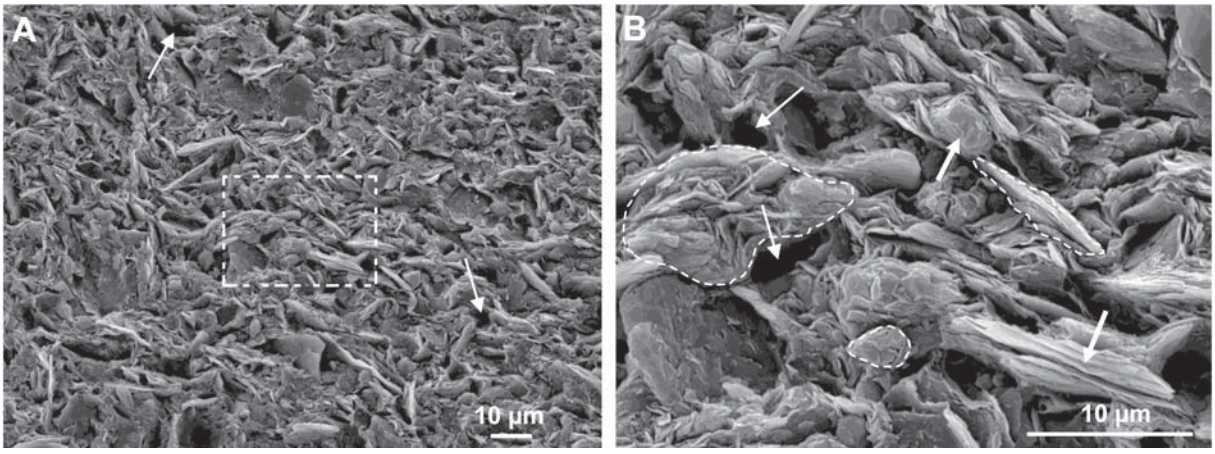

Text-fig. 3. Microstructures of clays – natural specimen. SEM images. Magnification of the images: A × 800, B × 3300. See text for explanations

intensity method (Smart and Tovey 1982; Sokolov 1990) and presented on a rose-diagram. Based on this diagram the anisotropic value of the microstructure anisotropy index K_a was determined and classified into one of the following groups:
– poorly-oriented microstructure K_a 0–7%,
– medium-oriented microstructure K_a 7–22%,
– highly-oriented microstructure K_a 22–78%.

PRESENTATION OF TEST RESULTS

Physical properties

The soils used in the testing program were Neogene clays consisting of 37% silt and 63% clay (see Table 1), recovered from the depth of 8.0–8.6 m from natural ground level, in the Stegny locality in Warsaw (Text-fig. 1). According to the Unified Soil Classification System (USCS, according to ASTM D 2487-06), these soils can be classified as CH fat clays. The values of the remaining physical properties are shown in Table 1. Geological-engineering parameters of the Neogene clays from this area allow assigning them into a category of very cohesive soils, with high, very high or extremely high swelling and very high potential expansiveness (Kaczyński and Grabowska-Olszewska 1997; Izdebska-Mucha and Wójcik 2014). The physical parameters of the soil pastes prepared for the analyses have similar values of the index parameters as the natural soils from the green clays level, which point to its natural grain size composition but changed structure and moisture.

The mineralogy of the clays was determined by X-ray diffraction (XRD) and thermal analysis (DTA) (Text-fig. 2). From a mineralogical point of view, the clays are mainly composed of clay minerals and quartz. Furthermore, X-ray analysis demonstrated small quantities of illite, which was not found in the thermal analysis. The results of the derivatographic analyses showed that the tested soils are polymineral sediments with the mineral composition of the clay fraction including the dominating beidellite (50.0%), which is a mineral from the smectite group with strong hydrophilic properties, kaolinite reaching 14.5%, and no illite. The second most abundant mineral is quartz and its content together with the thermally inactive material reaches 28.3%. Moreover, goethite is present in 7.2%. The results show a quantitative predominance of the minerals of the smectite group, specifically beidellite, and are therefore coherent with the beidellite type of clay in the Poznań series from the Warsaw region (Wyrwicki 1998).

Microstructural changes – qualitative analyses

The results of qualitative microstructural analyses of clays with natural (undisturbed) structure and clay pastes are presented in Text-figs 3–5.

Clays with undisturbed structure – natural specimens

The studied green clays are characterized by a matrix microstructure. This matrix is built of clay microaggregates and aggregates arranged in a disorderly fashion (Text-fig. 3A). Inclusions of small

grains of silt can be observed in the clay matrix (marked with a thick upper arrow in Text-fig. 3B). The clay matrix is tightly packed. The clay structural elements differ in size between 2–10 μm and have mostly an anisometric shape (shown with a dotted line in Text-fig. 3B). The clay particles in the microaggregates are arranged in parallel order accordingly to the face-to-face type (F–F) (as shown by a thicker lower arrow in Text-fig. 3B). Lack of orientation of structural elements can be seen (compare Text-fig. 3A with Text-fig. 5A and 5B). The pore space chiefly includes small microaggregate pores of 3–5 μm diameter, and isometric and anisometric shapes (thin arrows in Text-fig. 3A and 3B).

Initial paste

The initial paste shows a honeycomb microstructure, composed of polygonal, isometric pores (cells) (Text-fig. 4A). The cell walls are built of clay particles and microaggregates. The cells form isometric micropores with a diameter of 3–6 μm (thick arrows). The structure is very loosely packed. The clay microaggregates most often show an edge-to-edge (E–E) (upper thin arrow) and face-to-edge (F–E) (lower thin arrow) types of contact. In some places the clay microaggregates are bound into larger structural elements – aggregates characterized by stronger packing (delineated by a dotted line). Lack of orientation of structural elements can be seen. In some places, clay microaggregates show poor orientation, being connected into long lines of aggregates (upper thin arrow).

Paste under imposed suction of 100 kPa

The honeycomb microstructure of the initial paste underwent significant changes in this stage. Larger structural elements are more common, whereas the smaller elements are much fewer. As a result of the binding of microaggregates, larger structural elements – aggregates – were created (delineated by a dotted line). Loosely packed clay microaggregates in the initial paste have formed more strongly packed aggregates (compare elements delineated in Text-fig. 4A and 4B). The resulting accumulations of microaggregates branch out radially. Quantitative and qualitative changes in the pore space have also been recorded. Large micropore cells diminished their size to approx. 2 μm (thin arrows), whereas smaller pores became completely closed. Large micropores with a diameter of 7–10 μm (thick arrows) were formed. The clay microaggregate commonly have F–E types of contact (upper thick arrow). There is no specific orientation of the structural elements.

Paste under imposed suction pressure of 200 kPa

In this stage the microstructure has changed very distinctly, from honeycomb to matrix (Text-fig. 4C). The matrix microstructure is built of a clay mass (matrix) with inclusions of singular silty grains. This clay matrix is formed of microaggregates and clay aggregates (delineated by a dotted line), which are loosely packed. The clay microaggregates mostly have an F–F type of contact, but sometimes F–E and E–E types of contact also occur. The pore space is formed of large, isometric pores between the aggregates (thick arrows), and small, isometric pores between the microaggregates (thin arrows) and inside the microaggregates. There is no specific orientation of the structural elements.

Paste under imposed suction pressure of 300 kPa

In this state (Text-fig. 4D), the microstructure changed insignificantly in comparison with that for the paste under suction pressure of 200 kPa. The intensity of packing of the structural elements slightly increased. The micropores have changed their form from isometric to anisometric (thick arrow). The orientation of structural elements and the number of F−F contacts increased (thin arrow). The microstructure has become better oriented.

Paste under imposed suction pressure of 400 kPa

In comparison with the previous paste the intensity of packing of the structural elements increased significantly and the matrix microstructure changed into medium-packed (Text-fig. 4E). The pore space became homogenous. Larger micropores disappeared, and the pore space includes only smaller pores with a diameter of 1–2 μm (thick arrows). Most common are F−F type contacts (thin arrows). The microstructure became better oriented.

Paste under imposed suction pressure of 1600 kPa

The microstructural images of the paste under a suction pressure of 400 kPa and 1600 kPa are very similar. A large number of small micropores became closed and the microstructure became tightly packed (Text-fig. 4F). The number of F−F type contacts increased.

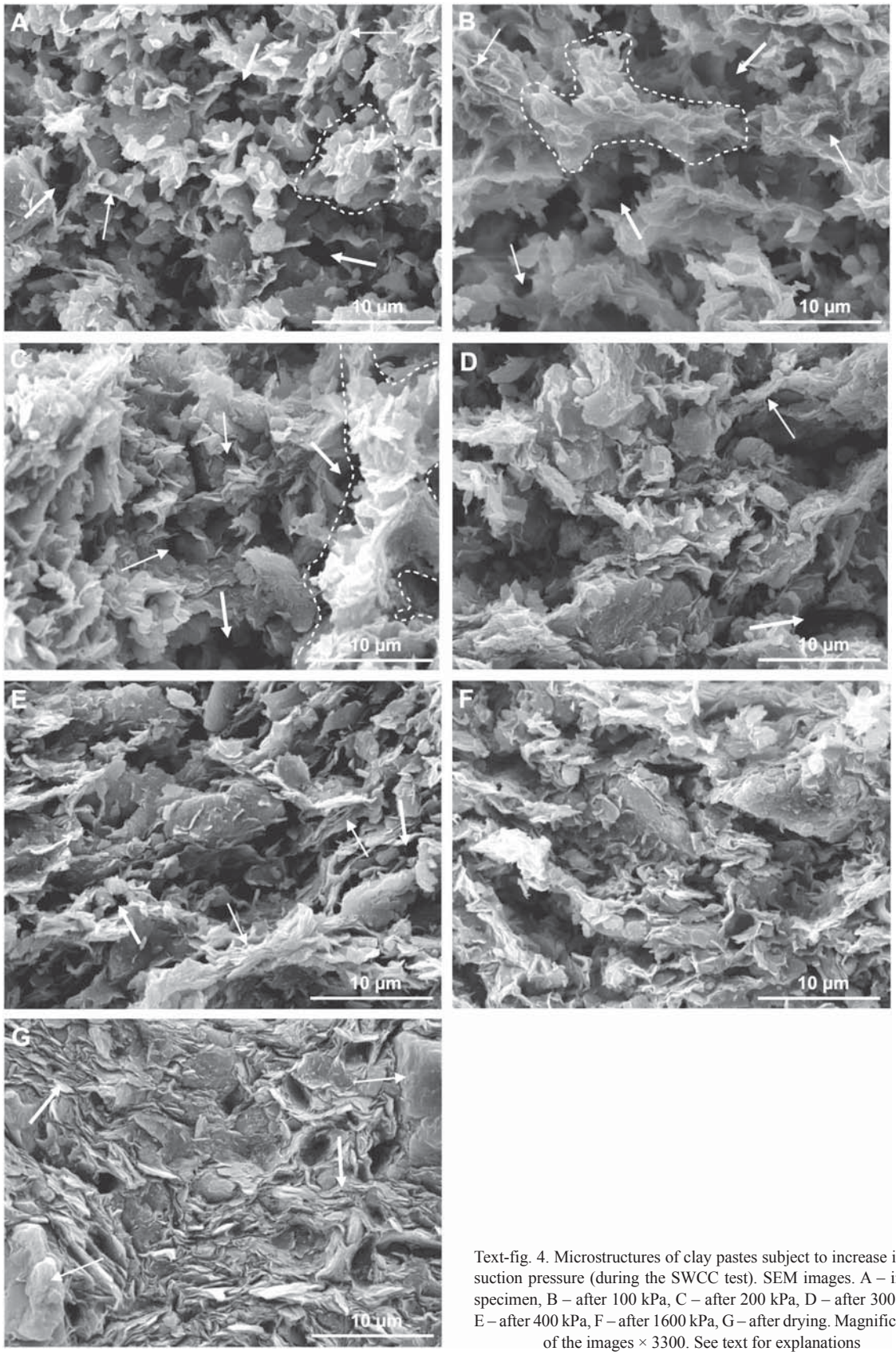

Text-fig. 4. Microstructures of clay pastes subject to increase in the suction pressure (during the SWCC test). SEM images. A – initial specimen, B – after 100 kPa, C – after 200 kPa, D – after 300 kPa, E – after 400 kPa, F – after 1600 kPa, G – after drying. Magnification of the images × 3300. See text for explanations

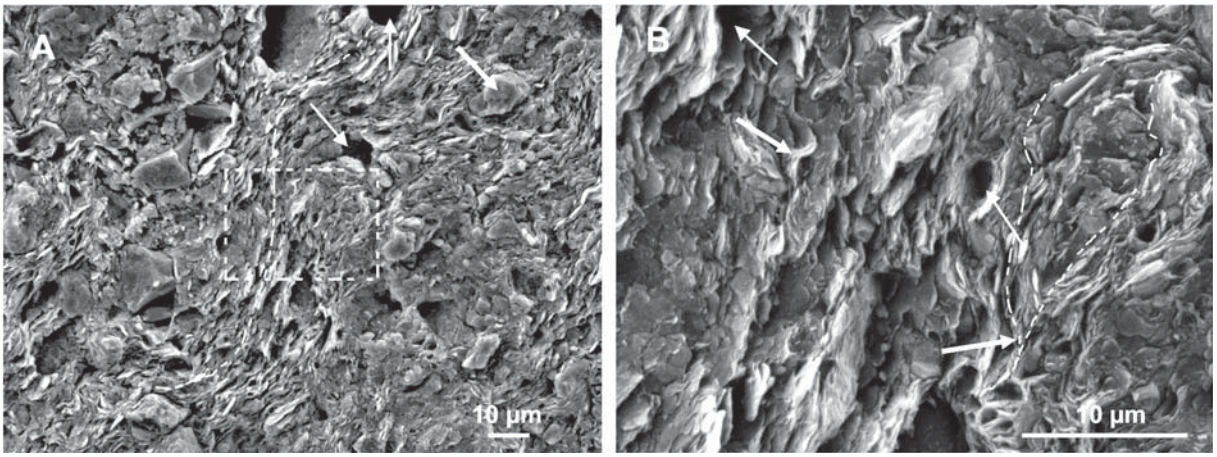

Text-fig. 5. Microstructures of clay pastes after shrinking. SEM images. Magnification of the images: A × 800, B × 3300. See text for explanations

Dried paste

After completion of all stages of the SWCC tests and drying, the microstructural image of the paste is very different in comparison with the images from the previous stages (Text-fig. 4G). Another change of the microstructure has occurred – from matrix to turbulent. The clay mass forms directed 'streams' of particles and microaggregates in horizontal and diagonal orientations (thick arrows). Singular grains of silt can be observed in the matrix (thin arrows). The clay mass is strongly packed and distinctly oriented. The clay particles tightly surround silty grains. The F–F and E–E types of contacts prevail. Anisometric and fissure-like pores dominate between tightly packed clay microaggregates with F−F orientation of the particles. The microstructure is highly organized.

Shrunken paste

The microstructural image of the paste presents a turbulent microstructure similar to that of a dried paste. The clay microaggregates are arranged in a turbulent way (thick arrows in Text-fig. 5B). Singular accumulations of fine silty grains are tightly surrounded by the clay matrix (thick arrow in Text-fig. 5A). The clay mass shows a directed, slightly wavy arrangement of structural elements (delineated by a dotted line in Text-fig. 5A and 5B). The F–F and E–E type contacts prevail between the clay microaggregates. Tightly packed clay microaggregates of F–F orientation of particles form anisometric and fissure-like smaller micropores with a diameter of 3–5 µm (thin arrows in Text-fig. 5B). Larger isometric micropores with a diameter of 10 **µ**m have also been observed (thin arrows in Text-fig. 5A). The microstructure is highly oriented. Rapid drying of the paste in the shrinkage process led to the creation of the same type of the microstructure as that observed in the dried paste, which systematically lost its moisture during the increase in suction pressure followed by drying (compare with Text-fig. 4G). However, a higher degree of packing and higher level of orientation can be observed in the shrunken paste.

Microstructural changes – quantitative analyses

The results of the SEM microstructural quantitative analyses of clays and pastes are presented in Table 2. Clays with undisturbed structure display a low value of porosity (20.8%) and a smaller number of pores in comparison to the pastes. However, the maximum, minimum and average pore diameter, pore area, and pore perimeter are much higher in comparison to the parameters obtained from the pastes. Such significant differences cannot be observed in the case of the total pores area or the total pore perimeter. In comparison with the pastes, the clays contain abundant mesopores and very few micropores. Among the shapes the anisometric pores prevail in comparison with the isomeric or fissure-like pores, but their values are similar to those that have been obtained from pastes. The microstructure anisotropy index reaches a low value.

During the increase of suction pressure, which caused dehydration of the paste, the microstructural parameters changed. Values of porosity *n* decreased from 37.9% for the initial paste to 30.7% for the dried

Parameter	Clay – natural specimen	Clay pastes									Shrunken specimen
		initial specimen	50 kPa	100 kPa	200 kPa	250 kPa	300 kPa	400 kPa	1600 kPa	dried specimen	
Porosity n [%]	20.8	37.9	37.2	36.3	36.9	35.2	34.4	34.3	33.2	30.7	31.5
Number of pores $N \times 10^3$	5.87	137.6	124.7	111.4	268.9	231.8	250.7	234.9	220.1	510.1	47.22
Maximum pores diameter D_{max} [µm]	276.6	122.5	169.7	148.1	172.1	194.4	126.4	163.5	124.6	95.8	61.6
Minimum pores diameter D_{min} [µm]	5.3	0.2	0.2	0.2	0.2	0.2	0.2	0.2	0.2	0.2	0.2
Average pores diameter D_{av} [µm]	12.5	1.0	1.0	0.9	0.7	0.7	0.7	0.7	0.8	0.6	1.1
Total pores area $S_t \times 10^3$ [µm^2]	1490.2	880.8	871.8	851.3	858.7	826.8	792.0	803.3	752.2	679.9	182.4
Maximum pores area S_{max} [µm^2]	123293.7	12094.3	23067.0	18049.0	24220.9	22367.0	10978.9	15580.0	12408.4	7456.0	3069.7
Minimum pores area S_{min} [µm^2]	22.0	0.0	0.0	0.0	0.0	0.0	0.0	0.0	0.0	0.0	0.0
Average pores area S_{av} [µm^2]	257.9	6.6	7.2	7.9	3.6	3.7	3.2	2.9	3.5	1.3	4.2
Total pores perimeter $P_t \times 10^3$ [µm]	795.4	1111.3	1012.0	953.9	1478.2	1289.7	1450.4	1303.4	1352.2	2497.5	330.8
Maximum pores perimeter P_{max} [µm]	10593.3	5005.3	7449.6	6000.5	9165.9	9397.0	5203.1	6294.4	3994.7	2248.1	2155.1
Minimum pores perimeter P_{min} [µm]	21.7	1.1	1.3	1.4	1.1	1.2	1.2	1.2	1.2	1.0	1.2
Average pores perimeter P_{av} [µm]	136.8	8.2	8.2	8.8	5.8	5.7	5.9	5.7	6.2	4.9	8.8
Maximum form index of pores K_{fmax} [–]	0.973	0.969	0.819	0.963	0.956	0.967	0.963	0.968	0.966	0.967	0.956
Minimum form index of pores K_{fmin} [–]	0.006	0.031	0.038	0.072	0.028	0.024	0.029	0.030	0.018	0.003	0.022
Average form index of pores K_{fav} [–]	0.426	0.454	0.479	0.487	0.456	0.460	0.448	0.458	0.436	0.390	0.455
Dominaning orientation direction of pores α [°]	152.2	48.1	93.8	92.7	96.7	146.8	110.3	64.8	62.9	118.8	70.8
Microstructure anisotropy index K_a [%]	17.1	11.8	33.9	23.2	19.5	37.1	31.8	44.2	31.5	17.2	29.9
Degree of microstructure orientation	medium	medium	high	high	medium	high	high	high	high	medium	high
Mesopores 10<Ø<1000 µm [%]	90.3	77.4	81.8	82.9	77.1	79.6	74.8	78.0	68.5	47.5	55.9
Micropores 0.1<Ø<10 µm [%]	9.7	22.6	18.2	17.1	22.9	20.4	25.1	22.0	31.5	52.5	44.1
Fissure-like pores a/b>10 [%]	1.1	0.8	0.2	0.1	1.0	0.6	0.5	0.4	0.4	1.7	0.4
Anisometric pores 1.5<a/b<10 [%]	86.3	84.6	83.3	83.4	83.7	85.6	85.4	84.9	86.1	85.1	84.0
Isometric pores a/b<1.5 [%]	12.6	14.6	16.5	16.5	15.3	13.8	14.1	14.7	13.5	13.2	15.6

Table 2. Quantitative microstructural parameters of the tested clays. Abbreviations: Ø – the equivalent diameter of pores, a/b – the ratio between two most different dimensions of pores

paste. A similar tendency can be observed for the total, average and maximum pore area *S*, the average and maximum pore diameter *D*, and the average and maximum pore perimeter *P*. An opposite tendency can be observed for the number of pores *N* (the parameter increased four times) and for the total

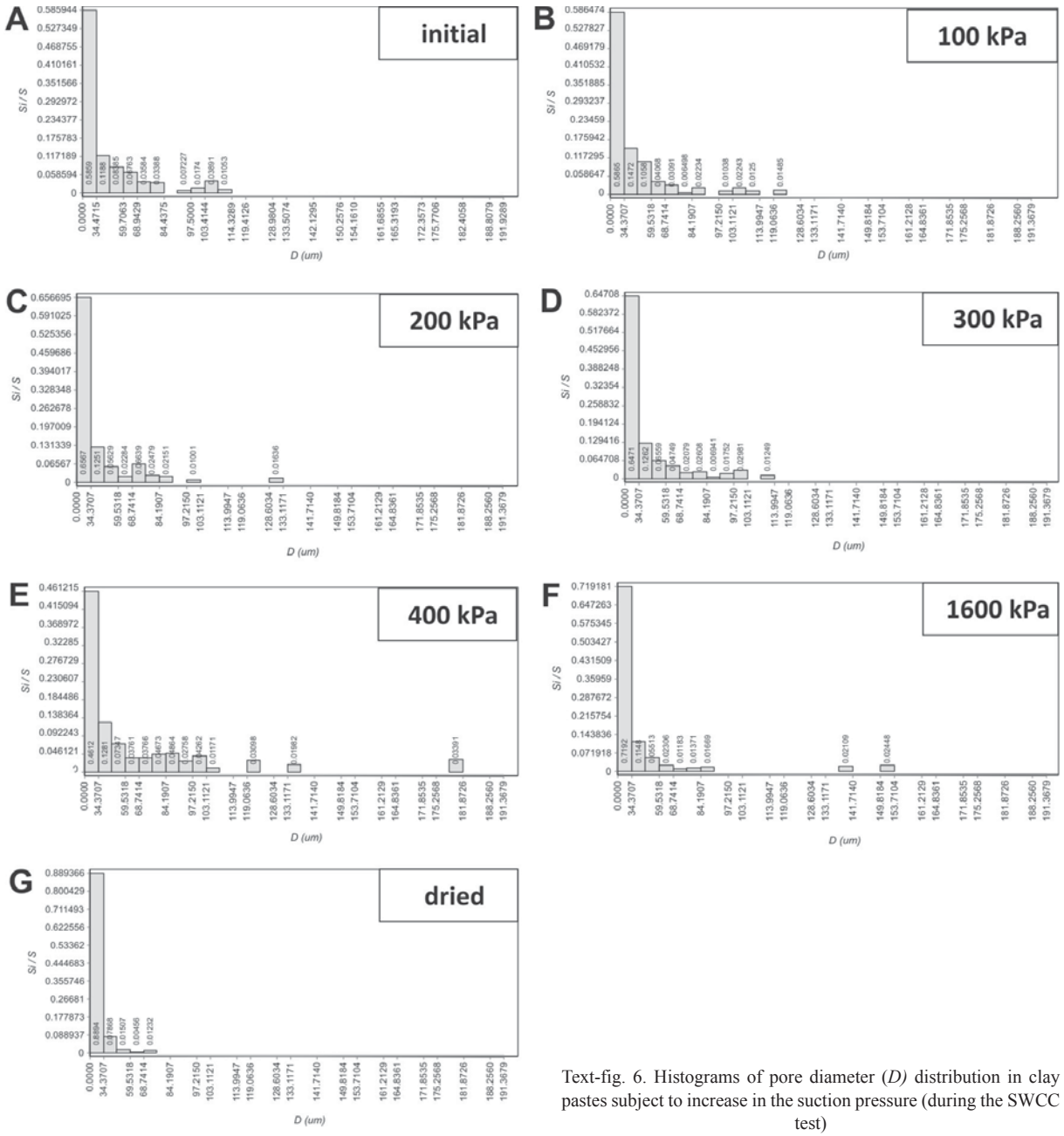

Text-fig. 6. Histograms of pore diameter (*D*) distribution in clay pastes subject to increase in the suction pressure (during the SWCC test)

pore perimeter *P* (the parameter increased twice). Significant changes have been observed in the distribution of pore shapes and sizes. As a result of dehydration under the increase in suction pressure, the number of the mesopores decreased and the number of micropores increased. For the minimum and average values of the pore form index K_f the decrease of value was observed during the water loss process. The fissure-like pores are least common in comparison with the isometric and anisometric ones (which are the most prevalent). The number of anisometric and fissure-like pores rises with increasing suction pressure. In turn, the number of isometric pores (which have a medium contribution) decreases with the increase of the suction pressure. With the increase of the suction pressure the microstructure anisotropy index K_a rises from 11.8% (medium-oriented microstructure) to 44.2% (highly-oriented microstructure).

Table 2 presents the results of quantitative analyses for the shrunken paste. In comparison with the paste dehydrated in stages, the morphometric parameters have undergone the most significant change.

Even though the shrunken paste has a similar porosity, the number of pores N is ten times smaller. Similarly, the average pore diameter, the total and maximum pore area, and total pore perimeter have smaller values in comparison to the dried paste. The increase of the minimal pore diameter was almost fivefold. Other morphometric parameters were at similar levels as in the dried paste sample.

The distribution of pore diameters D for the analyzed pastes has been presented in a set of histograms (Text-fig. 6). The initial paste shows a bimodal distribution of pore diameter. The paste under a suction pressure of 100 kPa is characterized by increase of the number of pores with a small diameter; in this case the range of pore sizes with larger diameters becomes wider, but their number decreases. The number of medium-sized pores also decreases. Under a suction pressure of 200 kPa the number of smaller pores still increases and most of the larger pores disappear (only singular larger pores are present). Under a suction pressure of 300 kPa the increase of the number of small pores and the decrease of the number of larger pores continues. Further increase of suction pressure to 400 kPa causes an increase of the number of medium-sized pores and a decrease of the number of smaller pores, and the appearance of a new class of very large pores. A suction pressure of 1600 kPa removed a large number of medium-sized pores and some classes of large pores in favour of the increase in the number of small-sized pores. In dried paste all large-sized and almost all medium-sized pores became closed, whereas the number of small-sized pores significantly increased.

The changes of the pore shapes in succeeding stages of dehydration of the paste under increasing suction pressure are presented in histograms (Text-fig. 7). The number of isometric pores systematically decreases during the process of water loss, and the distribution changes from bimodal to anisometric pores (compare Text-fig. 7A and 7G). The number of anisometric pores systematically increases with the change towards more fissure-like pores. Their distribution changes from multimodal (Text-fig. 7B) into asymmetric unimodal (Text-fig. 7G). Fissure-like pores are the least common although their number increases.

Rose-diagrams of the pore orientation are presented in Text-fig. 8. The shape of the rose-diagram for the initial paste is almost isometric. During two succeeding stages of dehydration, under suction pressures of 100 and 200 kPa, the shape of the rose-diagram is slightly anisometric. However, under suction pressures of 300 and 400 kPa, the shape of the rose-diagram changes significantly and is strongly anisometric (more flattened). Under a suction pressure of 1600 kPa and in the case of the dried paste, the tendency reverses slightly towards a more isometric shape of the rose-diagram.

INTERPRETATION AND DISCUSSION

In the examined natural samples from the green clays lithostratigraphic level (sample S3; Text-fig. 1), the presence of a matrix microstructure was observed (Text-fig. 3). A similar type of microstructure (matrix-turbulent) was reported by Kaczyński (2003) in the clays from the same lithostratigraphic level. The small difference in the observed microstructures may be the result of, for example, the degree of advancement of the glaciotectonic processes or the consistency state, which is an actual degree of moisture expressed by the value of parameter I_L.

During the process of increased suction pressure, the microstructure of the soil pastes changed significantly (Text-fig. 4B–F). The initial paste with a moisture of about 1.5 w_L has a honeycomb microstructure, which changes slightly with the increase of suction pressure to 100 kPa. Under a suction pressure of 200 kPa the change becomes notable and the microstructure modifies from honeycomb into matrix. Further microstructural changes in the range of suction pressure at 200–1600 kPa reshape the matrix microstructure only in the intensity of its packing, from loose to tightly packed.

A very similar change was observed also in the clays studied by Wei *et al.* (2013). The authors of that study analyzed the microstructure of a montmorillonite-kaolinite paste during changing suction pressure. They noted significant changes in the microstructural images from the honeycomb microstructure at the minimum pressure of 1 kPa, through a strongly packed matrix microstructure under a pressure of 1500 kPa, to the matrix-turbulent microstructure under a pressure of 158 MPa (see fig. 6 in Wei *et al.* 2013).

Our data and their comparison with the available literature show that the process of dehydration combined with the increase of suction pressure during the SWCC test causes significant transformation of the microstructure of the soil pastes. The honeycomb microstructure in the initial paste was formed due to the high water content. At this stage we are dealing with coagulated types of bonds between the structural elements, in which the van der Waals forces (Osipow 1975) play the most important part. The water film around the clayey particles is of maximum thickness

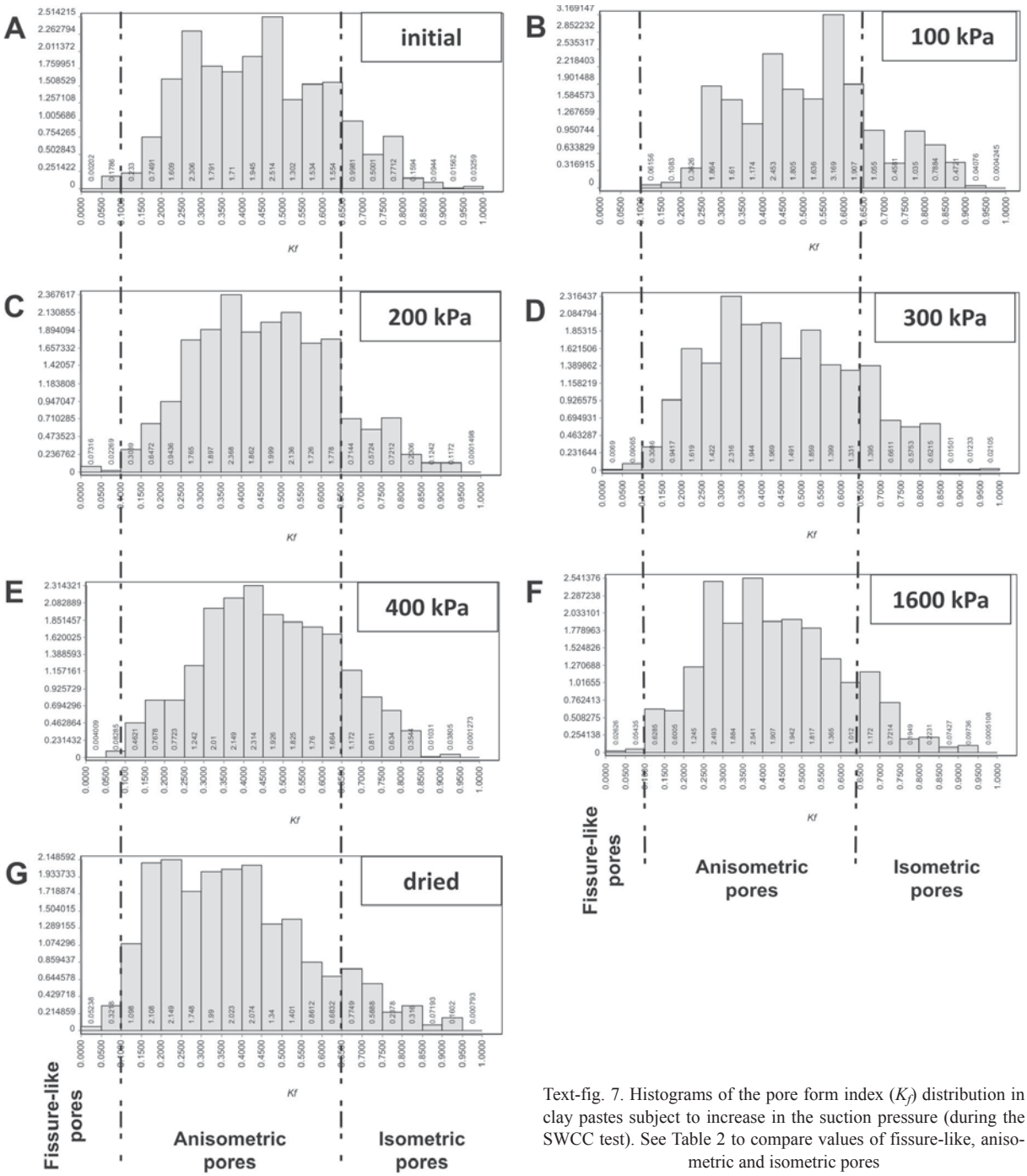

Text-fig. 7. Histograms of the pore form index (K_f) distribution in clay pastes subject to increase in the suction pressure (during the SWCC test). See Table 2 to compare values of fissure-like, anisometric and isometric pores

(strongly and poorly bound water), whereas loose water occurs in the pores between the elements of the mineral skeleton. As a result of the loss of moisture during the SWCC test, clay particles get closer together with the decrease of water content. The water film around the clay particles becomes thinner and ion-electrostatic forces start interacting on the contacts (Osipow 1975).

As a result of this process, a more strongly packed matrix microstructure is formed in the clay paste. With further water loss the water film starts breaking and chemical forces start interacting on the structural bonds (Osipow 1975). Clay particles start contacting one another directly on a very small area. Due to the action of the meniscus capillary forces, water still occurring in the corners of the pores causes a direct

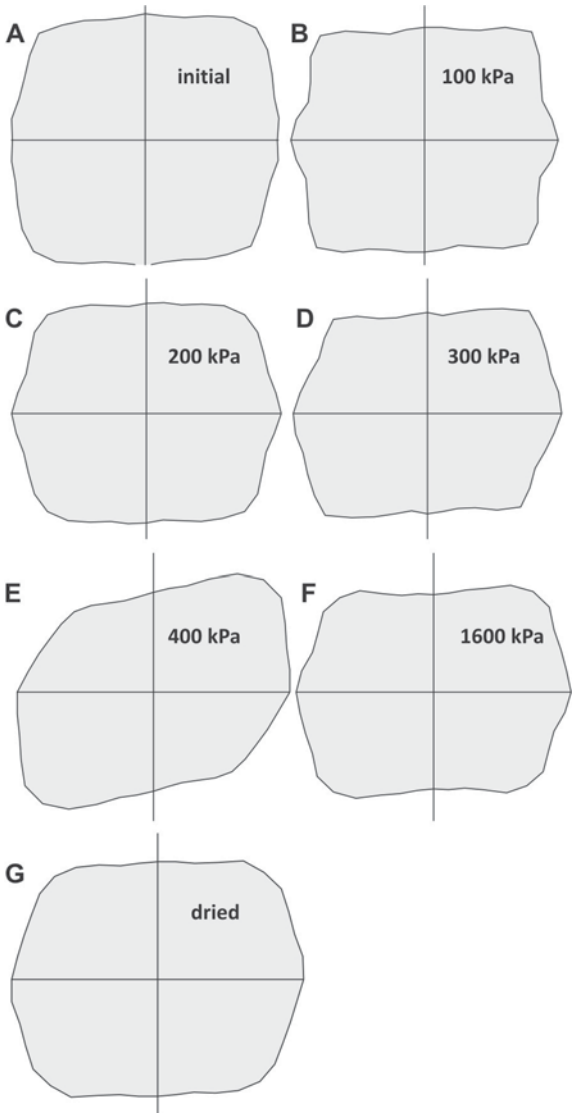

Text-fig. 8. Rose-diagrams of pore orientation (0–360°) in clay pastes subject to increase in the suction pressure (during the SWCC test). See Table 2 to compare values of microstructure anisotropy index K_a and degree of microstructure orientation

contact of increasingly larger areas of the clay particles. In the final stage of soil paste drying the loss of the strongly bound intralayer and interlayer water creates deformations that lead to bending of particles and clay microaggregates. As a result, a turbulent microstructure develops. A similar process of water loss in soils was observed by Viola *et al.* (2005) using an Environmental Scanning Electron Microscope (ESEM).

The turbulent microstructure occurring in the dried (Text-fig. 4G) and shrunken pastes (Text-fig. 5) developed due to the total water loss, without any consolidating pressure. The transition from the matrix microstructure into the turbulent microstructure during the process of increasing suction pressure was observed only during the final drying (Text-fig. 4B–F). Non-linear inner strains that started forming at the end of the drying phase were created by the meniscus capillary forces that formed a turbulent microstructure in the completely dried soil. It may be assumed that a similar process could have occurred in the Neogene clays that were studied by Kaczyński (2003), and the consistency state, i.e., the actual state of moisture of these clays, could represent a transitional, matrix-turbulent microstructure. So far undescribed (see Aylmore and Quirk 1960; Yong 1972; Grabowska-Olszewska *et al.* 1984), the observed microstructural changes that occurred during the performed SWCC test shed a new light on the processes of turbulent microstructure formation. According to the presented data it is clear that the processes of water loss due to the increase of suction pressures and additionally due to drying have a large influence on microstructural transformations, resulting in shrinking of clay soils. As an effect the turbulent microstructure is formed.

The microstructural changes described above have been analyzed in relation to the basic physical properties such as the liquidity index – I_L (Text-fig. 9). As reported by Kumor (2008), in natural conditions, Neogene clays in Poland have a liquidity index of 0.19 to -0.10 (averagely 0.03). According to Kaczyński (2003), who studied the overconsolidation and the microstructures in the Neogene clays from the Warsaw area, the liquidity index is -0.09 on the average. Text-fig. 9 illustrates the effect of suction on soil consistency including states from initial to dried. The transition of the analyzed Neogene clay paste from the liquid (I_L >1.0) to the solid state (I_L <0, after Head 1992) is accompanied by significant changes in the packing of the structural elements, along with simultaneous increase of suction pressure and drop in the liquidity index values (moisture loss). The initial paste with a moisture content above the value of the liquidity limit w_L has a honeycomb microstructure and is characterized by the highest liquidity index of 1.23. With an increase of the suction pressure to 100 kPa no significant microstructural changes were observed, however the analyzed paste transforms into a plastic state with a liquidity index of 0.6. The subsequent change of pressure to 200 kPa induces changes in the paste by forming a matrix microstructure with loose packing. The level of the liquidity index reduces to about 0.3. With an increase of suction pressure to 1600 kPa the matrix microstructure changes

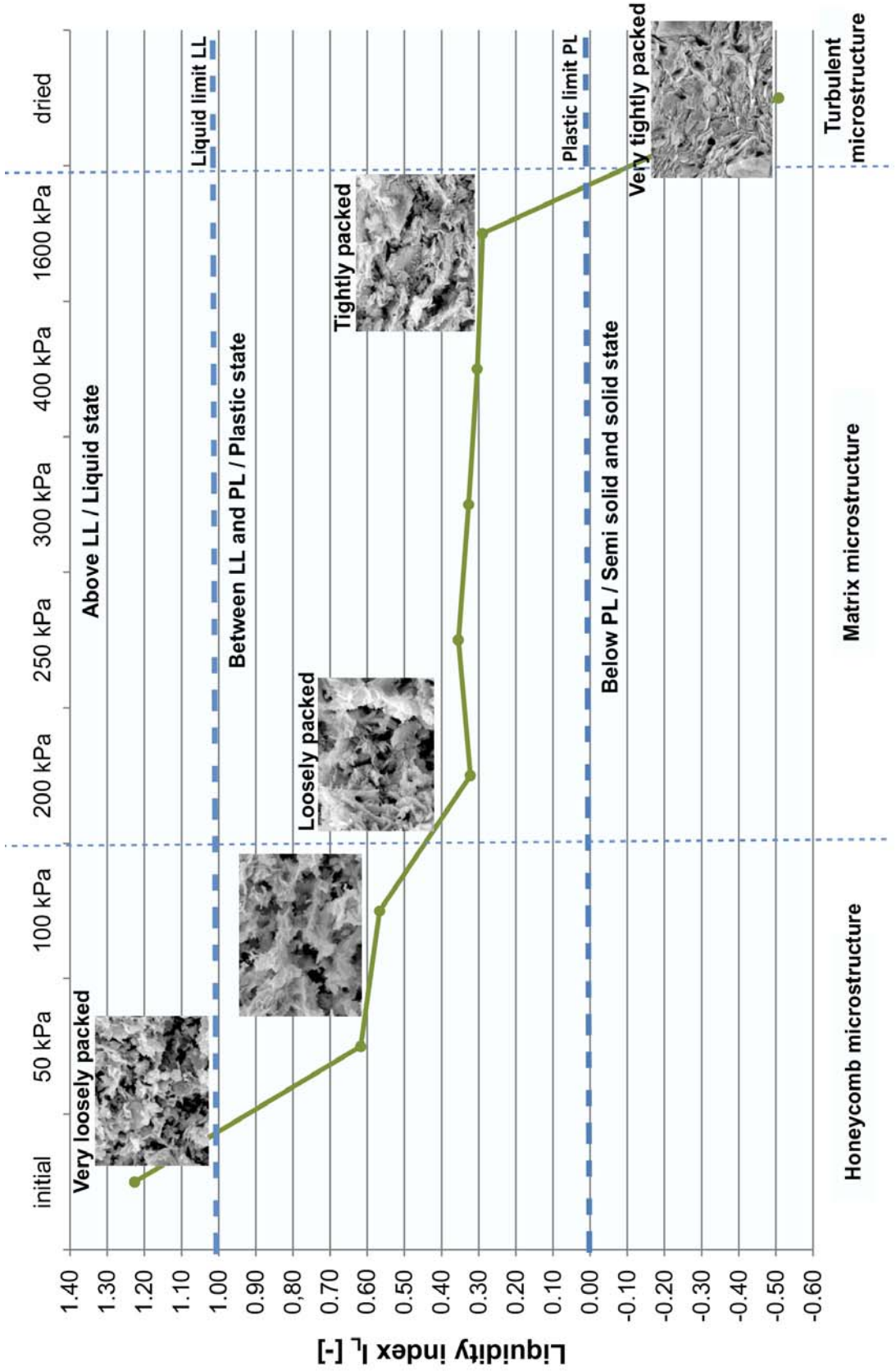

Text-fig. 9. Relationship between the level of plasticity I_L and increase in the suction pressure with microstructural changes

its packing from low to high, with the liquidity index remaining at the same level. Significant changes in the orientation and packing of the structural elements are observed in the dried sample. The turbulent microstructure and liquidity index of -0.57 indicate a solid state. The analysis of the natural clay sample and samples of similar clays studied by Kaczyński (2003) with a consistency around $I_L = 0$ indicates that they display a transitional, matrix-turbulent microstructure. Our analyses emphasize the correctness of the observed regularities during the gradual increase of suction pressure and the transition of the studied material from a liquid to a solid state. Therefore the water loss and the related microstructural transformation in the clay paste caused increase of the microstructure anisotropy index (Table 2).

The microstructural changes that co-occur with the soil moisture oscillations under the influence of the suction pressure depend on the soil behaviour during drying. The mineral composition of the clay fraction, especially the presence of hydrophilic minerals from the smectite group observed also in the studied clays, plays a particular role in these processes (Text-fig. 2). Strong hydrophilic properties of such minerals are crucial not only in the hydration process but also in the structural transformations connected with the dehydration process. Similar observations of the strong connection between the mineral composition and the soil behaviour forecasted in different water content conditions were made by Seiphoori *et al.* (2014). During the wetting and drying cycles, they observed a microstructural reorganization of bentonites rich in Na-smectites as a result of the interaction of the bentonite with the liquid phase present on the surfaces of phyllosilicate particles, infilling the free pores between them, and particularly bound within the phyllosilicate sheets. The loss of capillary water influenced the distribution of mesopores and micropores (Text-fig. 10). The results show that drying causes a reduction in the soil porosity from 37.9 to 30.7% (Table 2), corresponding mostly with reduction of the number of mesopores. An increase in the number of micropores, associated with this phenomenon, can also be observed.

The results of studies using the mercury porosimetry method are reported by Simms and Yanful (2001, 2002) and Koliji *et al.* (2006). The most significant changes are reported in pores with the diameter of 0.01−50 μm. During the increase in suction pressure the volume of pores with the diameter of 1–10 μm decreases, whereas the volume of the 0.1–1 μm and 10–50 μm pores increases. Additionally, a simultaneous increase in volume of small-size pores is observed in 0.1–1 μm pores. A similar process may be observed in the analyses of the clay pastes (Text-fig. 11). Analysis of histograms for the initial paste, through the subsequent values of suction pressure, to the dried paste shows that the contribution of the smallest pores, with a size range of 0–1 μm, increases significantly. This is particularly clear when comparing the sample that has undergone the suction pressure of 1600 kPa (4.1%) and the dried sample (11.2%). A similar regularity was not observed in the shrunken sample, whereas the soil with an undisturbed structure (natural) is completely devoid of such pores. These results may suggest that stronger internal strains occur during the paste shrinking (uncontrolled and rapid water loss). Such strains result in shorter distances between the structural elements and as a result closure of pores in this size range. The natural sample could have been subject to additional processes, which caused the disappearance of such pores.

The pores with a diameter of 1–10 μm also show a growing trend in volume. In the initial paste these pores contribute to 18.7%, with the most significant increase (up to 28.8%) under the suction pressure of 1600 kPa and in the dried paste (46.9%). Such significant increase cannot be observed in the shrunken paste, where it reaches only 42.1%, mostly due to the same reason as for the pores with a diameter of 0–1 μm. In the natural sample a small number (10.5%) of such pores can be observed, which is most likely due to the natural processes occurring in these sediments. The increasing trend in the 1–10 μm pores was not observed in the analyses using the mercury porosimetry method as reported by Simms and Yanful (2001, 2002) or Koliji *et al.* (2006). The samples for these analyses were dried using the freeze drying method, similarly as the samples for the qualitative and quantitative SEM analyses presented herein. However, the process of obtaining the results of porosity distribution differs significantly in both methods, which might have influenced the results.

During the quantitative microstructural analysis, the pore distribution was also analyzed (see rose-diagrams in Text-fig. 8). The orientation of the pore space has been subject to significant changes. For the initial paste and at initial suction pressures (100 and 200 kPa) the microstructure is medium-oriented. In turn, for the pastes under higher suction pressures the level of orientation increased and the microstructure became better oriented. Higher orientation of pores at increasing suction pressure was caused by the mobility of structural elements and them getting closer due to water loss. This also influenced the arrangement

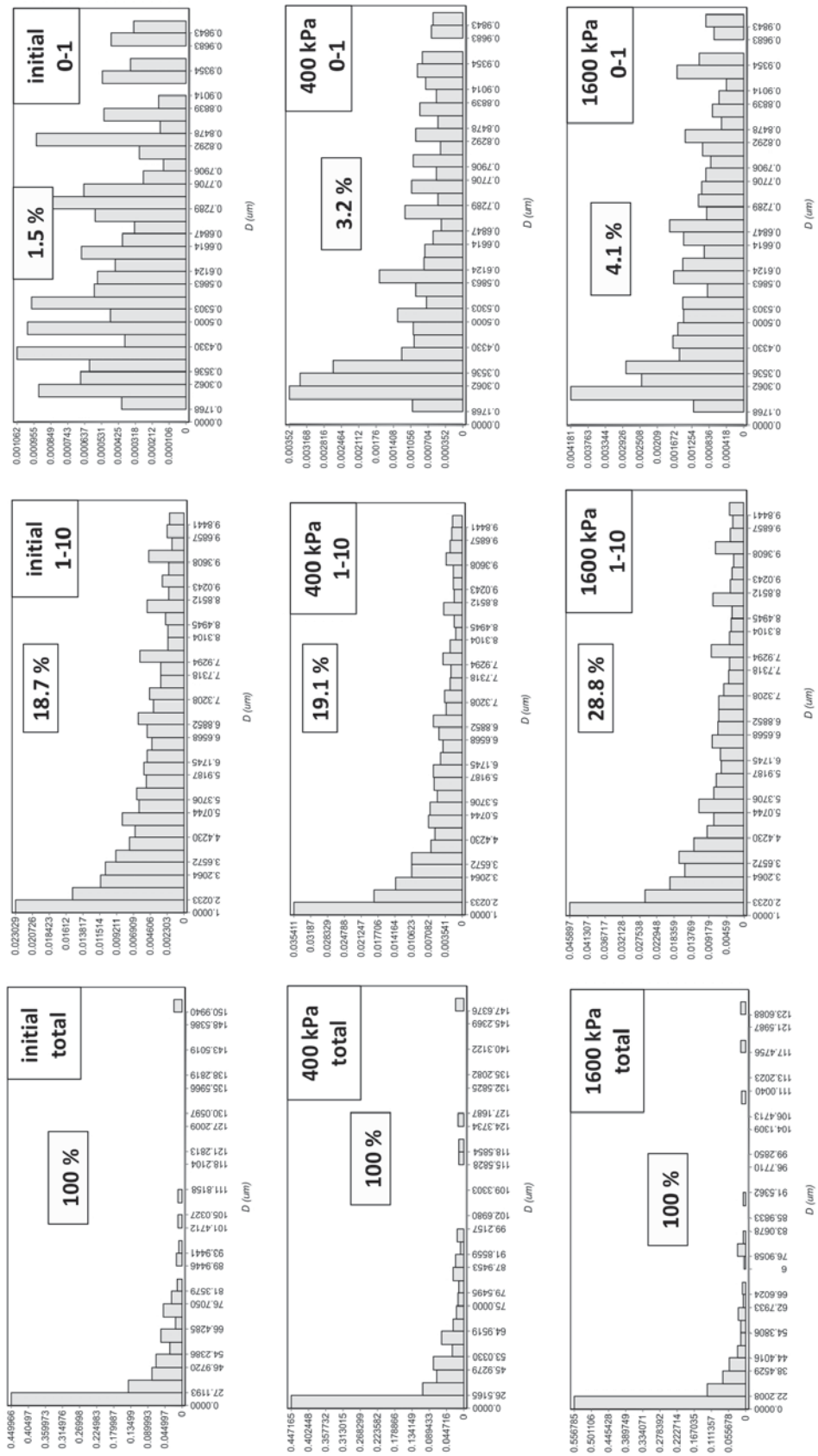

Text-fig. 10. Histograms of changes in pore diameter (D) distribution in clay pastes subject to increase in the suction pressure (during the SWCC test). Ranges of histograms: total ($0 - D_{max}$ µm), 1–10 µm, 0–1 µm

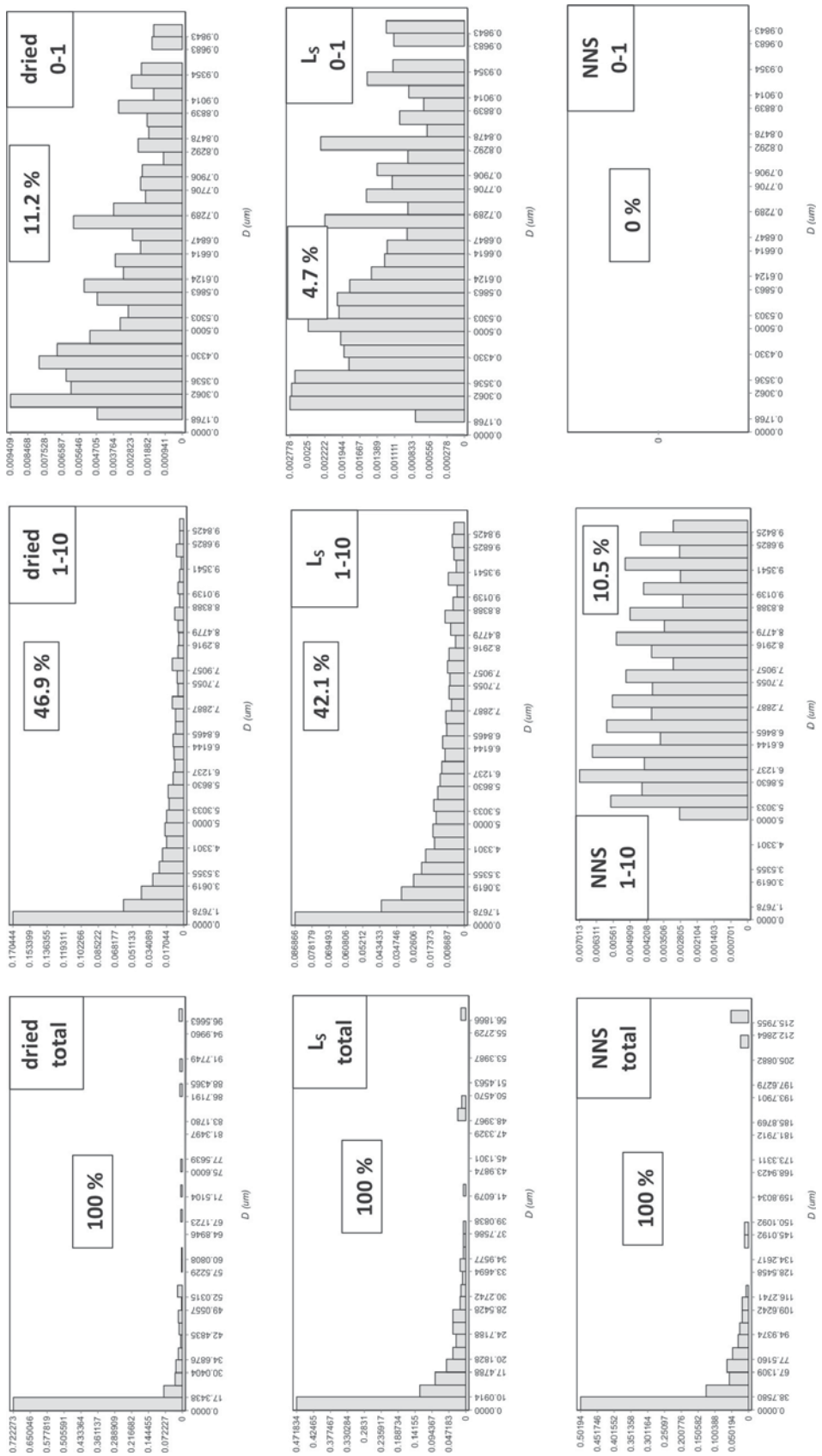

Text-fig. 10 – continuation

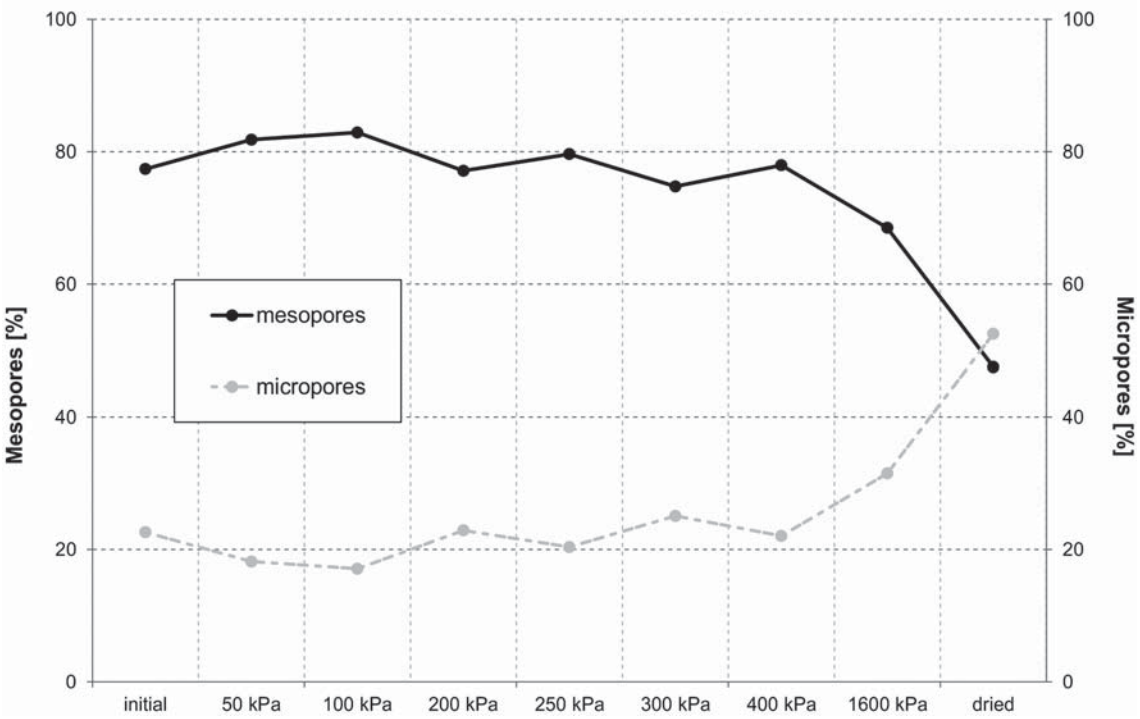

Text-fig. 11. Changes in the number of clay meso- and micropores with increase in the suction pressure (during the SWCC test)

of the pore space and the level of pore orientation. The pore shape changed from isometric to anisometric and fissure-like pores in the process of increase of suction pressure and water loss (Text-fig. 7). Wei *et al.* (2013) observed a similar trend in their study on the arrangement of clay particles in SEM images where their orientation increased along with the increase of suction pressure. Although the authors of that study studied the orientation of the clay mineral phase, but in this case, due to the platy habit of clay minerals, the comparison of the orientation of clayey particles and pores between them is justifiable.

CONCLUSIONS

Soil behaviour under diverse parameter-changing processes can be interpreted based on microstructural studies. This paper discusses the characteristics of the microstructure of Neogene clays from the Stegny locality in Warsaw, Poland: (i) in natural soils; (ii) in clay paste created as a result of stepwise increase of suction pressure; (iii) in dried paste created in the last stage of suction pressure, and shrunken paste; (iv) through quantitative analysis of the pore space geometry in all of the above mentioned cases; and (v) in relation to the results obtained due to the change of the soil plasticity.

The following conclusions can be drawn from the presented microstructural test results:

(1) The changes of soil moisture caused by the increase of suction pressure not only shape the plastic properties of soils but also significantly modify its structure (especially in the micro scale). During water loss, the initial soil paste in a liquid state changes its plasticity index, becoming a solid state. This is accompanied by the microstructural transformation from the honeycomb, through the matrix, to the turbulent microstructure. These changes are influenced e.g., by the soil behaviour during drying, taking into account the presence of water-sensitive clay minerals from the smectite group.

(2) The level of packing of the structural elements increased with the change of the type of microstructure. The honeycombcellular microstructure was characterized by a low level of packing (initial paste and paste under the suction pressure of 100 kPa); the matrix type of microstructure changed the level of packing from low to high (paste under the suction pressure of 200–1600 kPa), whereas the turbulent

microstructure had a high level of packing of the structural elements (dried and shrunken paste).

(3) With the increase of suction pressure, the type of microstructure changed from honeycomb through matrix to turbulent, which in turn shows an increase of its level of orientation from low to high.

(4) Under increasing suction pressure the total porosity of the studied pastes did not undergo significant transformations. In turn, the pore distribution changed. Significant modifications in the quantitative values of the morphometric and geometric parameters of pore space were also observed. In general, the values of morphometric parameters decreased with water loss. The pore space with larger, isometric pores transformed into a pore space with a domination of small, anisometric and fissure-like pores. The most significant changes were observed for pores with the diameter of 0–10 μm, where their contribution increased along with the increase in suction pressure. In the case of the shrunken sample, porosity did not change significantly, however a rapid shrinkage caused the decrease in the number of pores, in the maximum pore diameter and total pore perimeter. The process of rapid dehydration must have also been connected with closing of (especially very small) pores, which did not take place during the selective water loss under increase of suction pressure.

(5) The stepwise closure of the solid paste structure can be clearly observed in the process of water loss under increase of suction pressure.

Acknowledgements

The authors thank reviewers and editorial staff for comments on the text and its correction. The authors also thank Marek Baranski for samples of clay, which were obtained with the financial support of the research project KBN No. 12B 030 30 4T.

REFERENCES

Agus, S.S. and Schanz, T. 2005. Effect of shrinking and swelling on microstructures and fabric of a compacted bentonite-sand mixture. In: Bilsel, H. and Nalbantoglu, Z. (Eds), Proceedings of International Conference on Problematic Soils GEOPROB, vol. 2, pp. 543–550. Eastern Mediterranean University Press; Famagusta.

Aylmore, L.A.G. and Quirk, J.P. 1960. Domain or turbostatic structure of clays. *Nature*, **187**, 1046–1048.

ASTM D 2487-06. Standard Practice for Classification of Soils for Engineering Purposes (Unified Soil Classification System). American Society for Testing and Materials; Philadelphia.

Bajda, M. 2002. Application of static-seismic soundings in the assessment of mechanical parameters of soil, 110 p. Unpublished Ph.D. thesis, Warsaw University of Life Sciences; Warsaw. [In Polish]

Barański, M. and Wójcik, E. 2007. Assessment of the ability to deformation changes of Miocene and Pliocene clays from the study area. *Geologos*, **11**, 413–420. [In Polish]

Barański, M. and Wójcik, E. 2008. Estimation of ability to volume changes of Mio–Pliocene Clay from Warsaw. *Geologija*, **50** (Supplement), S49–S54.

Barański, M., Kaczyński, R., Borowczyk, M., Kraużlis, K., Trzciński, J., Wójcik, E., Granacki, W., Szczepański, T. and Zawrzykraj, P. 2004. Assessment of Pliocene clay behaviour from the Stegny site in effective strain conditions. Projekt badawczy KBN Nr 5 T12B 041 22, 280 p. Archiwum NCN; Warsaw. [In Polish]

Barański, M., Kaczyński, R., Borowczyk, M., Wójcik, E., Trzciński, J., Szczepański, T., Gawriuczenkow, I., Mieszkowski R., Kraużlis, K., Zawrzykraj, P., and Granacki, W. 2009. Assessment of structure anisotropy and effective strain in Miocene–Pliocene clays from the Stegny study site in Warsaw. Projekt badawczy KBN Nr 4T12B 030 30, 463 p. Archiwum NCN; Warsaw. [In Polish]

Bennet, R.H., Bryant, W.R. and Hulbert, M.H. (Eds) 1991. Microstructure of fine-grained sediments. From mud to shale, 582 p. Springer-Verlag; New York.

Brykczyńska, E. and Brykczyński, M. 1974. Geology of the Trasa Łazienkowska excavation in relation to the disturbances of Tertiary and Quaternary sediments in Warsaw. *Prace Muzeum Ziemi*, **22**, 199–216. [In Polish]

BS 1377-2:1990:6.5. Methods of test for soils for civil engineering purposes. Part 2: Classification tests.

Burland, J.B. 1990. On the compressibility and shear strength of natural clays. *Géotechnique*, **40**, 329–378.

Collins, K. and McGown, A. 1974. The form and function of microfabric features in a variety of natural soils. *Géotechnique*, **24**, 223–254.

Cuisinier, O. and Laloui, L. 2004. Fabric evolution during hydromechanical loading of a compacted silt. *International Journal for Numerical and Analytical Methods in Geomechanics*, **28**, 483–499.

Dananaj, I., Frankovska, J. and Janotka, I. 2005. The influence of smectite content on microstructure and geotechnical properties of calcium and sodium bentonites. *Applied Clay Science*, **28**, 223–232.

Delage, P. and Lefebvre, G. 1984. Study of the structure of a sensitive Champlain clay and of its evolution during consolidation. *Canadian Geotechnical Journal*, **21**, 21–35.

Dyjor, S. 1992. Development of sedimentation and process of sediment transformation in the Poznań series basin in Poland. *Prace Geologiczno-Mineralogiczne*, **26**, 3–18. [In Polish]

Fityus, S. and Buzzi, O. 2009. The place of expansive clays in

the framework of unsaturated soil mechanics. *Applied Clay Science*, **43**, 150–155.

Frankowski, Z. and Wysokiński, L. 2000. Engineering-geological atlas of Warsaw, 80 p. Archiwum CAG; Warszawa. [In Polish]

Gens, A. and Alonso, E.E. 1992. A framework for the behavior of unsaturated expansive clays. *Canadian Geotechnical Journal*, **29**, 1013–1032.

Geremew, Z., Audiguier, M. and Cojean, R. 2009. Analysis of the behavior of a natural expansive soil under cyclic drying and wetting. *Bulletin of Engineering Geology and the Environment*, **3**, 421–436.

Gillott, J.E. 1970. Fabric of Leda clay investigated by optical, electron-optical, and x-ray diffraction methods. *Engineering Geology*, **4**, 133–153.

Gillott, J.E. 1979. Fabric, composition and properties of sensitive soils from Canada, Alaska and Norway. *Engineering Geology*, **14**, 149–172.

Gillott, J.E. 1987. Clay in engineering geology, 468 p. Elsevier; Amsterdam, Oxford, New York, Tokyo.

Grabowska-Olszewska, B. 1975. SEM analysis of microstructures of loess deposits. *Bulletin of Engineering Geology and the Environment*, **11**, 45–48.

Grabowska-Olszewska, B. (Ed.) 1998. Properties of unsaturated soils, 217 p. PWN; Warszawa. [In Polish]

Grabowska-Olszewska, B., Osipov, V.I. and Sokolov, V.N. 1984. Atlas of the microstructure of clay soils, 414 p. PWN; Warszawa.

Gratchev, I.B., Sassa, K., Osipov, V.I. and Sokolov, V.N. 2006. The liquefaction of clayey soils under cyclic loading. *Engineering Geology*, **86**, 70–84.

Hattab, M. and Fleureau, J.M. 2010. Experimental study of kaolin particle orientation mechanism. *Getotechnique*, **60**, 323–331.

Hattab, M. and Fleureau, J.M. 2011. Experimental analysis of kaolinite particle orientation during triaxial path. *International Journal for Numerical and Analytical Methods in Geomechanics*, **35**, 947–968.

Hattab, M., Bouziri-Adrouche, S. and Fleureau, J.M. 2010. Èvolution de la microtexture d'une matrice kaolinitique sur chemin triaxial axisymètrique. *Canadian Geotechnical Journal*, **47**, 38–48.

Head, K.H. 1992. Manual of Soil Laboratory Testing. Vol. 1: Soil classification and compaction tests, 388 p. Pentech Press; London.

Hicher, P.Y., Wahyudi, H. and Tessier, D. 2000. Microstructural analysis of inherent and induced anisotropy in clay. *Mechanics of Cohesive-frictional Materials*, **5**, 341–371.

Izdebska-Mucha, D. and Trzciński, J. 2008. Effects of petroleum pollution on clay soil microstructure. *Geologija*, **50**, S68–S74.

Izdebska-Mucha, D. and Wójcik, E. 2014. Expansivity of Neogene clays and glacial tills from Central Poland. *Geological Quarterly*, **58**, 281–290.

Izdebska-Mucha, D., Trzciński, J., Żbik, M.S. and Frost, R.L. 2011. Influence of hydrocarbon contamination on clay soil microstructure. *Clay Minerals*, **46**, 47–58.

Kaczyński, R. 2000. Microstructural parameters of the pore space and some physical properties of selected cohesive soils from Warsaw. Materiały Sesji Jubileuszowej, pp. 143–149. Polish Academy of Sciences, Warsaw. [In Polish]

Kaczyński, R. 2001. Permeability, swelling and microstructure of Pliocene clays from Warsaw. In: Adachi, K. and Fukue, M. (Eds), Clay Sciences for Engineering, pp. 281–284. Proceedings of the International Symposium on Suction, Swelling, Permeability and Structure of Clays. Balkema; Shizuoka.

Kaczyński, R. 2003. Overconsolidation and microstructures in Neogene clays. *Geological Quarterly*, **47**, 43–54.

Kaczyński, R. and Grabowska-Olszewska, B. 1997. Soil mechanics of the potentially expansive clays in Poland. *Applied Clay Science*, **11**, 337–355.

Kaczyński, R., Grabowska-Olszewska, B., Borowczyk, M., Ruszczyńska-Szenajch, H., Kraużlis, K., Trzciński, J., Barański, M., Gawriuczenkow, I. and Wójcik, E. 2000. Lithogenesis, microstructures and engineering-geological properties of Pliocene clays in the Warsaw region. Projekt badawczy KBN Nr 9T12B 005 16, 127 p. Archiwum NCN; Warsaw. [In Polish]

Katti, D.R. and Shanmugasundaram, V. 2001. Influence of swelling on the microstructure of expansive clays. *Canadian Geotechnical Journal*, **38**, 175–182.

Koliji, A., Laloui, L., Cuisinier, O. and Vulliet, L. 2006. Suction induced effects on the fabric of a structured soil. *Transport in Porous Media*, **64**, 261–278.

Kulesza-Wiewióra, K. 1990. Preparation of smaples for mineralogical and physical-chemical analyses. In: Grabowska-Olszewska, B. (Ed.), Metody badań gruntów spoistych, pp. 130–141. Wydawnictwa Geologiczne; Warszawa. [In Polish]

Kumor, M.K. 2008. Selected geotechnical problems of expansive clays in the area of Poland. *Architecture Civil Engineering Environment*, **1**, 75–92.

Kumor, M.K. 2016. Expansive clays in the construction basement from Bydgoszcz. Selected geotechnical problems, 235 p. Wydawnictwo UTP; Bydgoszcz. [In Polish]

Lech, M. and Bajda, M. 2004. Identification of geological barriers at the Stegny site. 16th European Young Geotechnical Engineers Conference, pp. 201–210. Austrian Society for Engineers and Architects; Vienna.

Lloret, A., Romero, E. and Villar. M.V. 2004. FEBEX II Project. Final report on thermo-hydro-mechanical laboratory tests. Ref. PT-10/04. ENRESA, Dirección de Ciencia y Tecnología; Madrid.

McGown, A. and Collins, K. 1975. The microfabrics of some expansive and collapsing soils. Proceedins of 5th Panamerican Conference, Vol. 1, pp. 323–332. Soil Mechanics and Foundation; Buenos Aires.

Mitchell, J.K. 1976. Fundamentals of soil behavior, 422 p. John Wiley and Sons; New York.

Murphy, C.P., Bullock, P. and Biswell, K.J. 1977. The measure-

ment and characterization of voids in soil thin sections by image analysis. Part II applications. *Journal of Soil Science*, **28**, 509–518.

Osipov, V.I. 1975. Structural Bonds and the Properties of Clays. *Bulletin of Engineering Geology and the Environment*, **12**, 13–20.

Osipov, V.I., and Sokolov, V.N. 1978a. A study of the nature of the strength and deformation properties of clay soils with the help of the scanning electron microscope. *Bulletin of Engineering Geology and the Environment*, **17**, 91–94.

Osipov, V.I. and Sokolov, V.N. 1978b. Relation between the microfabric of clay soils and their origin and degree of compaction. *Bulletin of Engineering Geology and the Environment*, **18**, 73–81.

Osipov, V.I. and Sokolov, V.N. 1978c. Structure formation in clay sediments. *Bulletin of Engineering Geology and the Environment*, **18**, 83–90.

Osipov, V.I., Nikolaeva, S.K. and Sokolov, V.N. 1984. Microstructural changes associated with thixotropic phenomena in clay soils. *Géotechnique*, **34**, 293–303.

Piwocki, M. 2002. Evolution of ideas on the stratigraphy of the Poznań Formation in the Polish Lowlands. *Przegląd Geologiczny*, **50**, 255. [In Polish]

PN-86/02480. Building soils. Definitions, symbols, sub-division and description of soils. [In Polish]

PN-88/B-04481. Building soils. Analysis of soil samples. [In Polish]

Pusch, R. 1966. Quick-clay microstructure. *Engineering Geology*, **1**, 433–443.

Pusch, R. 1970. Microstructural changes in soft quick clay at failure. *Canadian Geotechnical Journal*, **7**, 1–7.

Romero, E., Gens, A. and Lloret, A. 1999. Water permeability, water retention and microstructure of unsaturated Boom clay. *Engineering Geology*, **54**, 117–127.

Romero, E., Hoffmann, C., Castellanos, E., Suriol, J. and Lloret, A. 2005. Microstructural changes of compacted bentonite induced by hydro-mechanical actions. Proceedings of International Symposium on Large Scale Field Tests in Granite, Sitges, Spain, 12–14 November 2003. In: Alonso, E.E. and Ledesma, A. (Eds), Advances in understanding engineered clay barriers, pp. 193–202. Taylor, Francis Group; London.

Ruszczyńska-Szenajch, H., Trzciński, J. and Jarosińska, U. 2003. Lodgement till deposition and deformation investigated by macroscopic observation, thin-section analysis and electron microscope study at site Dębe, central Poland. *Boreas*, **32**, 399–415.

Schmitz, R.M., Schroeder, C. and Charlier, R. 2005. Influence of microstructure on geotechnical properties of clays. *Unsaturated Soils: Experimental Studies*, **93**, 89–100.

Seiphoori, A., Ferrari, A. and Laloui, L. 2014. Water retention behaviour and microstructural evolution of MX-80 granular bentonite during wetting and drying cycles. *Géotechnique*, **64**, 721–734.

Sergeyev, Y.M., Grabowska-Olszewska, B., Osipov, V.I. and Sokolov, V.N. 1978. Types of the microstructures of clayey soils. Proceedings of the III International Congress I.A.E.G., 4–8 September, pp. 319–327. International Association of Engineering Geology; Madrid.

Sergeyev, Y.M., Grabowska-Olszewska, B., Osipov, V.I., Sokolov, V.N. and Kolomenski, Y.N. 1980. The classification of microstructures of clay soil. *Journal of Microscopy,* **120**, 237–260.

Sergeyev, Y.M., Spivak, G.V., Sasov, A.Y., Osipov, V.I., Sokolov, V.N. and Rau, E.I. 1984a. Quantitative morphological analysis in a SEM-microcomputer system – I. Quantitative shape analysis of single objects. *Journal of Microscopy*, **135**, 1–12.

Sergeyev, Y.M., Spivak, G.V., Sasov, A.Y., Osipov, V.I., Sokolov, V.N. and Rau, E.I. 1984b. Quantitative morphological analysis in a SEM-microcomputer system – II. Morphological analysis of complex SEM images. *Journal of Microscopy*, **135**, 13–24.

Simms, P.H. and Yanful, E.K. 2001. Measurement and estimation of pore shrinkage and pore distribution in a clayey till during soil-water characteristic curve tests. *Canadian Geotechnical Journal*, **38**, 741–754.

Simms, P.H. and Yanful, E.K. 2002. Predicting soil-water characteristic curves of compacted plastic soils from measured pore-size distributions. *Géotechnique*, **52**, 269–278.

Simms, P.H. and Yanful, E.K. 2004. A discussion of the application of mercury intrusion porosimetry for the investigation of soils, including an evaluation of its use to estimate volume change in compacted clayey soils. *Géotechnique*, **54**, 421–426.

Simms, P.H. and Yanful, E.K. 2005. A pore-network model for hydromechanical coupling in unsaturated compacted clayey soils. *Canadian Geotechnical Journal*, **42**, 499–514.

Smart, P. and Tovey, K. 1982. Electron microscopy of soils and sediments: techniques, 264 p. Clarendom Press; Oxford.

Sobolewski, M. 2002. Determination of characteristics of water flow in cohesive soils based on in situ analyses, 85 p. Unpublished Ph.D. thesis. Archiwum SGGW; Warsaw. [In Polish]

Sokolov, V.N. 1990. Engineering-geological classification of clay microstructures. Proceedings of the 6th International Congress IAEG, pp. 753–760. Balkema; Rotterdam.

Sokolov, V.N., Yurkovets, D.I. and Razgulina, O.V. 2002. Stiman (Structural Image analysis): a software for quantitative morphological analysis of structures by their images (User's manual. Version 2.0), 75 p. Laboratory of Electron Microscopy, Moscow State University; Moscow.

Szczepański, T. 2005. Assessment of the consolidation state of selected clays based on the analysis of compressibility parameters, 148 p. Unpublished Ph.D. thesis, Faculty of Geology, University of Warsaw; Warsaw. [In Polish]

Tovey, N.K. and Wong, W.K. 1973. The Preparation of Soil and Other Geological Material for the SEM, pp. 59–69. International Symposium of Soil Structure; Gothenburg.

Trzciński, J. 2004. Combined SEM and computerized image

analysis of clay soils microstructure: technique and application. In: Jardine, R.J., Potts, D.M. and Higgins, K.G. (Eds), Advances in geotechnical engineering: The Skempton conference, pp. 654–666. Thomas Telford; London.

Trzciński, J. 2008. Microstructure and physico-mechanical properties of tills in Poland. *Geologija*, **50**, S26–S39.

Villar, M.V. and Lloret, A. 2001. Variation of the intrinsic permeability of expansive clays upon saturation. In: Adachi, K. and Fukue, M. (Eds), Clay Science for Engineering, pp. 259–266. A.A. Balkema; Rotterdam.

Viola, R., Tuller, M., Or, D. and Drasdis, J. 2005. Microstructure of clay-sand mixtures at different hydration states. Proceedings of International Symposium on Advanced Experimental Unsaturated Soil Mechanics, Trento, Italy, 27–29 June 2005. In: Tarantino, A., Romero, E. and Cui, Y.J. (Eds), Advanced experimental unsaturated soil mechanics, pp. 437–442. Taylor and Francis Group; London.

Wei, X., Hattab, M., Fleureau, J.M. and Hu, R. 2013. Micro-macro experimental study of two clayey materials on drying paths. *Bulletin of Engineering Geology and the Environment*, **72**, 495–508.

Wójcik, E. 2003. Influence of suction pressure on the permeability of selected cohesive soils from Warsaw, 131 p. Unpublished Ph.D. thesis, University of Warsaw; Warsaw. [In Polish]

Wyrwicki, R. 1998. Mineral composition of clays of the Poznań series in the Warsaw region, 10 p. Zakład Prac Geologicznych, Wydział Geologii UW, Warszawa; Warsaw. [In Polish]

Wyrwicki, R. and Kościówko, H. (Eds) 1996. Methods of clay deposit analysis, pp. 56–76. Państwowy Instytut Geologiczny; Warszawa–Wrocław. [In Polish]

Yong, R.N. 1972. Soil technology and stabilization. *Proceedings of the 4th Asian Regional Conference on Soil Mechanics and Foundation Engineering*, **2**, 111–124.

Yong, R.N. 2003. Influence of microstructural features on water, ion diffusion and transport in clay soils. *Applied Clay Science*, **23**, 3–13.

Zhang, G., Germaine, J.T. and Whittle, A.J. 2005. Drying induced alteration to the microstructure of a tropical soil. *Proceedings of* International Symposium on advanced experimental unsaturated soil mechanics, Trento, Italy, 27–29 June 2005. In: Tarantino, A., Romero, E. and Cui, Y.J. (Eds), Advanced experimental unsaturated soil mechanics, pp. 443–449. Taylor and Francis Group; London.

Manuscript submitted: 15th October 2017
Revised version accepted: 15th January 2019